Build Simul (2020) 13: 387–399
https://doi.org/10.1007/s12273-019-0582-9

Numerical investigation on thermophoretic deposition of particles in turbulent duct flow with conjugate heat transfer: Analysis of influencing factors

Hao Lu, Li-zhi Zhang (✉), Rong-rong Cai

Key Laboratory of Enhanced Heat Transfer and Energy Conservation of Education Ministry, School of Chemistry and Chemical Engineering, South China University of Technology, Guangzhou 510640, China

Abstract

Thermophoretic deposition of particles in turbulent duct flow is of significant relevance in energy and thermal engineering applications. However, conjugate heat transfer (CHT) was commonly not considered in the previous studies, but may have crucial influences on particle deposition behaviors. Therefore, thermophoretic particle deposition in turbulent duct flow with and without CHT was numerically investigated by using $\overline{v'^2}-f$ turbulence model and discrete particle model (DPM) with a modified discrete random walk method. After grid independence study and numerical verification, several important influencing factors on particle deposition velocity were studied, such as flow Reynolds number, temperature difference between inlet hot air and cool wall, thermal conductivity ratio and width ratio of solid and fluid domain. The thermophoresis greatly increases deposition velocity of small particles but has no influence on large particles. The critical particle relaxation time τ_{p}^{+} for thermophoresis effect is 20, which is the same for all the cases in this study. The corresponding particle diameter is 28 μm. The thermophoretic deposition is enhanced when the flow Reynolds number and temperature difference between air and wall increase. This is because the wall-normal temperature variety is higher for large Reynolds number and temperature difference, which can enhance thermophoretic deposition. However, CHT reduces the thermophoretic deposition by decreasing temperature difference in fluid region. Besides, higher thermal conductivity ratio and width ratio of solid and fluid domain will decrease the thermophoretic deposition, as thermal conduction in solid domain becomes more intense.

Keywords

particle deposition,
conjugate heat transfer,
influencing factors

Article History

Received: 3 December 2018
Revised: 9 September 2019
Accepted: 12 September 2019

1 Introduction

Thermophoretic deposition of particles in turbulent duct flow is a basic and crucial process in numerous energy and thermal engineering applications, such as building ventilation system, air cleaner, heat exchanger and powdered coal burner (Zhao et al. 2008; Olufade and Simonson 2018; Chen et al. 2018). During particle deposition process with thermophoresis, conjugate heat transfer (CHT) always occurs between fluid domain and solid wall domain, which may have significant influences on the thermal distribution of turbulent flow and also particle deposition characteristics. However, very limited studies considered the effects of CHT on thermophoretic particle deposition in duct flow. Therefore, the objective of this paper is to investigate thermophoretic deposition of particles in duct airflow with CHT, as it is of great significance on a large number of engineering applications.

The fundamental research on particle deposition commonly considered vertical turbulent duct flow without thermophoresis. The process is mainly determined by several influencing factors including the forces on particles, turbophoresis, the Brownian and turbulent diffusion (Shimada et al. 1993; Lai 2002; Zhang 2015). However, particle deposition behaviors are greatly modified with the increase of particle relaxation time. When particle relaxation time is low, the Brownian and turbulent diffusions are the dominant mechanisms on particle deposition. Nevertheless, turbulent eddies and particle inertia become significant for deposition

E-mail: Lzzhang@scut.edu.cn

List of symbols

A	area of particle deposition	t_d	time period of dust deposition
B	thickness of solid wall	T_s	temperature of solid domain
C_C	Cunningham correction factor	T_f	ttemperature of fluid domain
C_0	mean particle concentration	U_{mean}	mean velocity of air
C_D	drag coefficient of particle	U_{free}	freestream velocity of air
C_{ps}	specific pressure heat of solid wall	u_g	velocity of fluid
d_p	diameter of dust particle	u_p	velocity of particle
f	an elliptic equation for the relaxation function	u^*	frictional velocity of air
f_c	fanning friction factor	v'	wall-normal fluctuating velocity of air
g	gravitational acceleration	$\overline{v'^2}$	wall-normal stress of flow
H	width of half duct	V	volume of duct flow
J	particle deposition number	V_d	particle deposition velocity
k	turbulent kinetic energy	V_d^+	dimensionless particle deposition velocity
K_c	Saffman's lift force coefficient	ρ_g	density of fluid
N_d	number of dust deposited on the walls	ρ_p	density of particle
N_0	total particle number	ρ_s	density of solid wall
Re	Reynolds number	ζ	normal distributed random number
Re_p	particle Reynolds number	ν	kinetic viscosity of air
s_{ij}	deformation tensor	τ	particle relaxation time
S	ratio of particle-to-fluid density	Δt	time step
S_0	spectral intensity of a Gaussian white noise random process	λ_s	thermal conductivity of solid domain
		λ_f	thermal conductivity of fluid domain
S_E	volumetric heat source in solid domain	τ_p^+	dimensionless particle relaxation time

characteristics with the increase of particle relaxation time. Finally, particle inertia is the main factor to control deposition process when particle relaxation time is large enough (Bakanov 1991; Cheng 1997; Sippola and Nazaroff 2004; Zhao and Wu 2006).

When temperature difference presents in the airflow fields, particles would experience a thermophoretic force and the force direction is toward the colder side. Thermophoretic particle deposition is widely encountered in numerous thermal and energy engineering application and was attracted much attentions of researchers (Romay et al. 1998; Lee et al. 2006; Wang et al. 2011; Lu and Lu 2017). Lee et al. (2006) experimentally investigated thermophoresis of small particles in turbulent duct flow. The results showed that thermophoretic deposition is a dominant mechanisms for deposition of small particles. Wang et al. (2011) measured thermophoretic deposition process of polydispersed particles in turbulent duct flow. A new prediction model was developed from the measurement results. Romay et al. (1998) studied thermophoresis in turbulent duct flow. The results showed that turbulent deposition is more important than thermophoresis for large particles.

Numerical simulation based on computational fluid dynamics (CFD) has becoming a powerful tool to study thermophoresis process of particles in turbulent flow (Lu and Lu 2015a, 2016). He and Ahmadi (1998) simulated particle thermophoresis in duct flow by the Reynolds-averaged Navier-Stokes equations (RANS) model and discrete particle model (DPM). It was found that deposition velocity obviously increases for small particle due to the thermophoretic deposition. Furthermore, Dong and Chen (2011) studied thermophoresis effect on particle deposition in turbulent duct flow by CFD. They found that thermophoretic deposition enhances particle deposition in the near-wall region of cold side. Liu et al. (2010) predicted thermophoresis of inhalable particles in turbulent flow. The results showed that thermophoretic deposition is crucial for small particle deposition. Thakurta et al. (1998) investigated thermophoretic deposition process in turbulent flow by direct numerical simulation (DNS). The results showed that turbophoresis and thermophoresis are both important for deposition characteristics.

Although thermophoresis of particles in turbulent duct flow was well studied by the previous researches, effects of CHT on particle deposition behaviors has been seldom investigated according to the authors' knowledge. However, the influence of CHT between the airflow and solid wall on particle deposition occurs in real engineering application

and needs to be well investigated. Therefore, this study aims to numerically investigate the thermophoretic deposition of particles in turbulent duct flow with CHT. Moreover, several important influencing factors on particle deposition behaviors were studied, such as flow Reynolds number, temperature difference between the inlet air and solid wall, the thermal conductivity ratio and width ratio of solid and fluid domain. Besides, the thermal fields in different cases were obtained and compared to analyze thermophoretic particle deposition.

2 Numerical methods

The ANSYS FLUENT 15.0 combined with user-defined function (UDF) code was adopted to predict thermophoretic deposition of particles in duct airflow with and without CHT, as its capacity and reliability have been widely proved by the a large number of previous researches (Zhang and Chen 2009; Majlesara et al. 2013).

2.1 Two-phase flow models

For airflow fields, the Reynolds-averaged Navier-Stokes equations (RANS) model were resolved to predict turbulent flow. The governing equations for the airflow are described as follows:

$$\frac{\partial \overline{u}_i}{\partial x_i} = 0 \tag{1}$$

$$\frac{\partial \overline{u}_i}{\partial t} + \overline{u}_j \frac{\partial \overline{u}_i}{\partial x_j} = -\frac{1}{\rho}\frac{\partial \overline{p}}{\partial x_i} + \frac{1}{\rho}\frac{\partial}{\partial x_j}\left(\mu \frac{\partial \overline{u}_i}{\partial x_j} - \rho \overline{u_i' u_j'}\right) \tag{2}$$

where $\overline{u}_i$ is the time-averaged velocity, $\overline{p}$ is the time-averaged pressure, μ is the dynamic viscosity of air. The $\overline{v'^2} - f$ model was developed by Durbin (1995) for predicting the anisotropy of Reynolds stresses and the wall-normal velocity fluctuation without using wall functions. The $\overline{v'^2} - f$ model was successfully used to predict thermophoretic deposition of particles in duct flow by Zhang and Chen (2009). Thus this turbulence model was adopted in the present study. The detailed $\overline{v'^2} - f$ governing equations can be found in the literature (Durbin 1995).

For particle motion, discrete particle model (DPM) was used to predict particle deposition behaviors by tracking trajectories of particles. As the particle concentration is dilute enough in this study (particle volume fraction is less than 10^{-6}), one-way coupling was used in the simulation. The effects of particle motions on airflow fields were ignored and particle-particle collisions were also neglected in the study. The particle motion equation can be written as follows (FLUENT 2009):

$$\frac{du_p}{dt} = \frac{1}{\tau}\frac{C_D Re_p}{24}(u_g - u_p) + \frac{g(\rho_p - \rho_g)}{\rho_p} + \zeta\sqrt{\frac{\pi S_0}{\Delta t}} + \frac{2\rho_g K_c \nu^{0.5}}{\rho_p d_p (S_{lk} S_{kl})} s_{ij}(u_g - u_p) + F_x \tag{3}$$

Drag coefficient C_D can be calculated by (FLUENT 2009):

$$C_D = \begin{cases} \dfrac{24}{Re_p} & \text{for } Re_p < 1 \\ \dfrac{24}{Re_p}(1 + 0.15 Re_p^{0.687}) & \text{for } 1 < Re_p < 400 \end{cases} \tag{4}$$

Particle deposition velocity was computed by (FLUENT 2009):

$$V_d = \frac{J}{C_0} = \frac{N_d / (t_d \cdot A)}{N_0 / V} \tag{5}$$

where J is particle deposition number. The non-dimensional deposition velocity can be computed by:

$$V_d^+ = \frac{V_d}{u^*} \tag{6}$$

where frictional velocity u^* can be calculated by:

$$u^* = \sqrt{\tau_w / \rho_g} = U_{mean}\sqrt{f/2} \tag{7}$$

where f is the fanning friction factor and is computed by:

$$f = 0.0791 \cdot Re^{-0.25} \quad (2{,}800 < Re < 10^5) \tag{8}$$

The non-dimensional particle relaxation time can be computed by:

$$\tau_p^+ = \frac{C_C S d_p^2 u^{*2}}{18\nu^2} \tag{9}$$

The most crucial influencing factors on deposition velocity include particle forces and turbulent flow fields. The main particle forces are drag force, pressure gradient force, Basset force, Brownian force, Saffman's lift force, virtual mass force and thermophoretic force. The magnitude of these particle forces were analyzed carefully by Zhao et al. (2004). They found that the drag force, Brownian force and Saffman's lift force are relatively large compared with the other forces. These three forces are taken into account in the present study. The thermophoretic force is mainly determined by the temperature gradient and particle mass. The influence of thermophoretic force is more intense for higher temperature gradient and smaller particle size, as shown in the following equation:

$$F_x = -D_{T,p}\frac{1}{m_p T}\frac{\partial T}{\partial x} \tag{10}$$

For turbulent flow fields, the flow structures and turbulent fluctuations defined by DRW are the main influencing factors for particle deposition. In our simple duct flow, the flow structures are not very complex and turbulent fluctuations are the dominate factor for particle deposition. It can be seen that the influence of turbulent fluctuation on particle deposition velocity (the so-called particle turbulent dispersion) is very important on particle deposition, especially for small particles (Tian and Ahmadi 2007; Gao et al. 2012; Lu and Lu 2015b). The radiation heat transfer was neglected in the study because the surface area of particle is quite small. This assumption was also adopted in many previous related literature (Majlesara et al. 2013).

2.2 Turbulent dispersion of particles

Turbulent dispersion of particles is crucial for particle deposition behaviors in turbulent flow. The discrete random walk model (DRW) was adopted to predict turbulent dispersion of particles. The isotropic DRW model considers turbulent velocity fluctuation by turbulent kinetic energy, as follows:

$$u_i' = \zeta_i\sqrt{2k/3} \tag{11}$$

where u_i' is the turbulent velocity fluctuation. ζ is a Gaussian random number with zero mean and unit variance. k is turbulent kinetic energy. It was found that over prediction of particle deposition velocity will be appeared by directly using the isotropic DRW model in duct flow, as the turbulent flow near the wall is intensely anisotropic (Tian and Ahmadi 2007; Gao et al. 2012). The $\overline{v'^2}-f$ model directly predicts the wall-normal velocity fluctuation, which is crucial for turbulent dispersion of particles. Therefore, this study adopted $\overline{v'^2}-f$ model to correct the isotropic DRW model. The corrected DRW model considering turbulent anisotropy can be described by (Zhang and Chen 2009):

$$u_\perp' = \zeta_\perp\sqrt{\overline{v'^2}} \tag{12}$$

$$u_\parallel' = \zeta_\parallel\sqrt{(2k-\overline{v'^2})}/2; \quad y^+ \le y^+_{\mathrm{Lim}} \tag{13}$$

$$u_i' = \zeta_i\sqrt{\overline{u_i'u_i'}} = \zeta_i\sqrt{2k/3}; \quad \text{otherwise} \tag{14}$$

where the subscripts $\perp$ and $\parallel$ represent the spatial coordinates normal or parallel to the wall, respectively. The y^+_{Lim} is the upper bound of the anisotropic region. y^+ is dimensionless distance from the wall, which can be defined as follows:

$$y^+ = \frac{yu^*}{\nu} \tag{15}$$

The instantaneous turbulent velocity fluctuation generated by the Eqs. (12)–(14) will be used for predicting turbulent dispersion of particles.

2.3 Conjugate heat transfer

The conjugate heat transfer was considered in the present study, as the thermal conduction in the solid domain may influencing thermophoretic deposition characteristics of particles in duct flow. The Fourier thermal conduction equation for solid region can be described as,

$$\frac{\partial}{\partial t}(\rho_s C_{ps} T_s) = \nabla\cdot(\lambda_s \nabla T_s) + S_E \tag{16}$$

where C_{ps} is the specific pressure heat of solid wall. λ_s is the thermal conductivity of solid domain. S_E is an option volumetric heat source, which is zero in this study. The conjugate boundary conditions on the interface of the fluid domain and solid domain can be written as

$$\lambda_s\left(\frac{\partial T_s}{\partial y}\right)_{y=0} = \lambda_f\left(\frac{\partial T_f}{\partial y}\right)_{y=0} \tag{17}$$

$$(T_s)_{y=0} = (T_f)_{y=0} \tag{18}$$

where $y = 0$ is the interface between airflow and inner solid wall.

2.4 Boundary conditions

The fully developed velocity distribution was adopted and imposed at inlet in ANSYS FLUENT by using UDF code, as follows (Tian and Ahmadi 2007):

$$U = U_{\mathrm{free}}\left(\frac{y}{H}\right)^{1/7} \quad \text{for} \quad y \le H \tag{19}$$

$$U_{\mathrm{free}} = \frac{8}{7}U_{\mathrm{mean}} \tag{20}$$

Moreover, fully developed TKE distribution was imposed at inlet (Tian and Ahmadi 2007):

$$k = \frac{\tau_w}{\rho_g\sqrt{C_\mu}} + \frac{y}{H}\left(0.002U^2_{\mathrm{free}} - \frac{\tau_w}{\rho_g\sqrt{C_\mu}}\right) \quad \text{for} \quad 0 \le y \le H \tag{21}$$

$$\tau_w = \frac{\rho_g U^2_{\mathrm{mean}}}{2}\cdot f_c \tag{22}$$

No-slip boundary condition was adopted on the wall. Pressure outlet condition was used in the outlet and symmetry

condition was employed in the upper boundary. Particles were released from duct inlet with uniform spatial distribution. The initial particle velocity was equal to the mean air velocity. Moreover, the escape condition was used in the upper and outlet boundary. Tian and Ahmadi (2007) investigated particle deposition in turbulent duct flow by CFD method. They assumed that particles will all deposit on the duct wall surfaces in the simulation. The results showed their numerical particle deposition velocity is in good agreement with the related experimental data. This is because the adhesion force is much larger than the rebound force when the particle velocity is small enough. The assumption was widely used in the CFD simulation of particle deposition under low airflow velocity (Tian and Ahmadi 2007; Zhang and Chen 2009; Gao et al. 2012; Majlesara et al. 2013; Lu and Lu 2015b). Thus particles were assumed to deposit on the wall when touch the wall surface in the present study.

3 Case description and solution strategy

3.1 Computational geometry

Schematic of thermophoretic particle deposition in duct airflow with and without CHT was shown in Fig. 1. Tian and Ahmadi (2007) investigated particle deposition in two-dimensional turbulent duct flow. The numerical results were in good agreement with the experimental data. Thus the two-dimensional gas-particle flow was predicted in the present study to reduce the computational cost. For the case without CHT, the length of the air duct was 0.5 m and the width of the duct was 0.01 m. As the flow is symmetric, only half of the duct was predicted to reduce the computational cost. The inlet airflow was hot while the wall was cool, as shown in the Fig. 1(a). The temperature of inlet air was 300, 350 or 400 K and the wall temperature was 300 K. Thus the temperature difference between inlet air and cool wall was 0, 50 or 100 K, respectively. When CHT was considered, the width ratio of solid and fluid domain B/H was 1, 2 or 4, respectively. The outer surface of the solid domain was 300 K. The inlet air velocity was 5 or 10 m/s, the corresponding Reynolds number was 3425 or 6850 based on inlet flow velocity and duct height, respectively. The thermal conductivity ratio of solids and fluids λ_s/λ_f was 1, 10 or 100, respectively. The dynamic viscosity of air was 1.789×10^{-5} kg/(m·s). The density of air is related to the temperature. The Boussinesq model is employed to consider the buoyancy effect. A total number of 15,000 particles were released from duct inlet. The particle-air density ratio S was 2,000. Particle size in the study was 1, 2, 3, 5, 10, 20, 30 or 50 μm. The corresponding particle relaxation time of 1 μm is 0.071.

3.2 Computational grids

Computational grids were developed to discretize airflow domain and solid wall domain, as shown in Fig. 2. The structured grids become fine in the near-wall region of the fluid flow while uniform grids were adopted for solid domain. Furthermore, a grid independence study was conducted to predict particle deposition velocity in duct flow without thermophoretic deposition and CHT, as displayed in Fig. 3(a). The grid number for coarse, medium and fine grids was 300×60, 400×70 or 500×80 respectively. It can be found that the deposition velocity profiles between the medium and the coarse grid cases are quite different. However, the particle

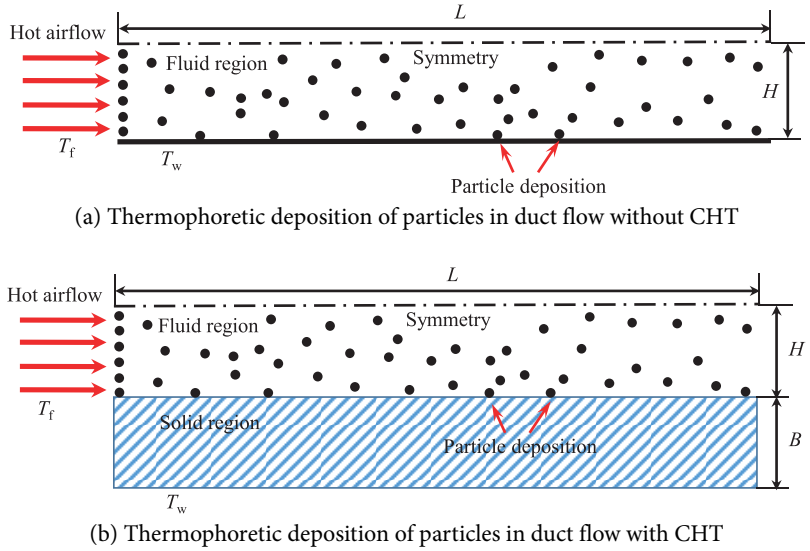

(a) Thermophoretic deposition of particles in duct flow without CHT

(b) Thermophoretic deposition of particles in duct flow with CHT

Fig. 1 Schematic of thermophoretic deposition of particles in duct flow with and without CHT

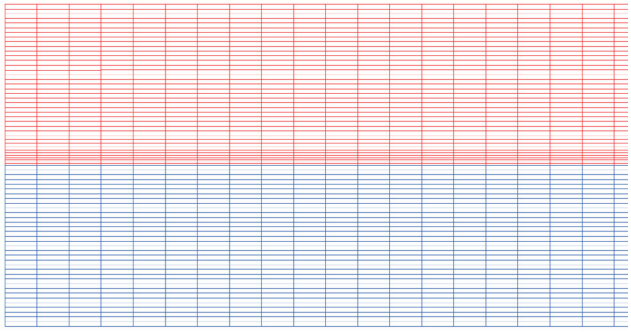

Fig. 2 Computational grids for fluid region and solid region

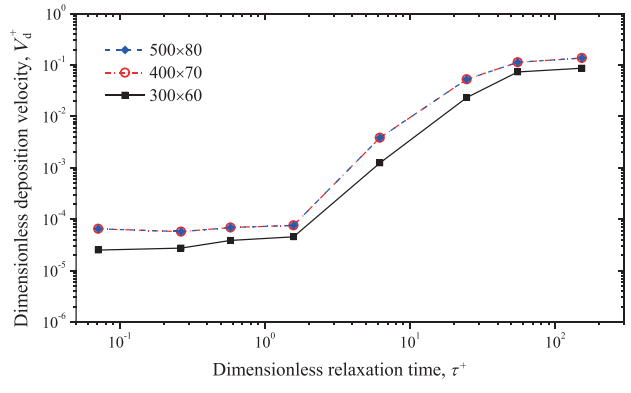

(a) Grid independence study for particle deposition velocity in duct flow

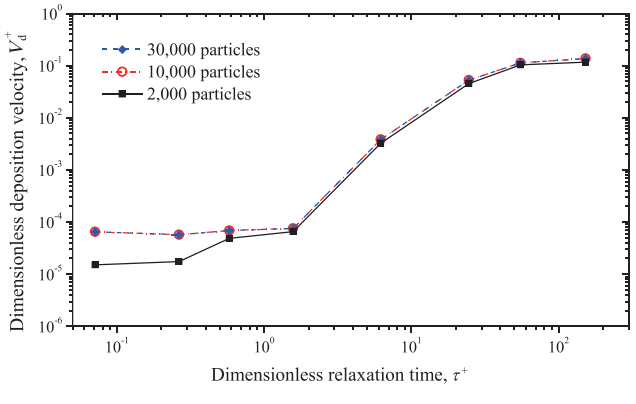

(b) Independence study of particle number for particle deposition velocity in duct flow

Fig. 3 Independence study of grid number and particle number on deposition velocity

deposition velocity profiles are almost the same between the medium and fine grid cases. Thus the fine grid was used in the study. The grid number was 40,000 for fluid domain and 30,000 for solid domain. Moreover, an independency test of particle number on particle deposition velocity was conducted as shown in the Fig. 3(b). It can be seen that the computational results are the same when particle number is larger than 10,000.

The DRW model was adopted in the simulation. The particle deposition velocity fluctuations can be obtained by repeating particle trackings. The results showed that the deposition velocities for large particles are almost not influenced by the turbulent fluctuation defined by DRW model due to the high particle inertia. However, the deposition velocities are little changed by the turbulent fluctuation for small particles.

3.3 Solution strategy

The governing equations of airflow were resolved by the finite volume method (FVM). The convection term and the diffusion terms were discretized by the second-order upwind scheme and the second-order central difference scheme, respectively. The SIMPLE algorithm (Partankar 1980) was used to decouple the velocity and pressure fields. The governing equation of particle motion was resolved by the Runge-Kutta scheme. The modified anisotropic particle-eddy interaction model as well as the fully developed velocity and TKE distributions in inlet were imposed into ANSSY FLUENT by UDF codes.

4 Results and discussions

4.1 Numerical validation

Particle deposition velocity profile in vertical duct airflow without thermophoretic depoisiton was obtained and compared with related literature's results (Friedlander and Johnstone 1957; Postma and Schwendiman 1960; Well and Chamberlain 1967; Liu and Agarwal 1974; El-Shobokshy 1983; Shimada et al. 1993; Lee and Gieseke 1994), as shown in Fig. 4. From the figure, particle deposition velocity firstly increases and then becomes invariable when particle diameter increases. Besides, the present deposition profile agrees well with the results collected from the literatures. Therefore, the present two-phase flow model as well as computational grids can accurately predict particle deposition characteristics in turbulent duct flow.

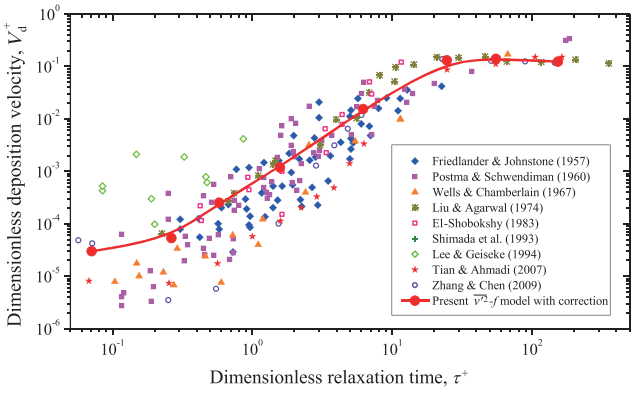

Fig. 4 Numerical validation of particle deposition velocity in turbulent duct flow

4.2 Effects of Reynolds number on particle deposition with and without CHT

Reynolds number has great influences on airflow fields and thermal distributions in duct flow, and then further affect particle deposition characteristics. Figure 5 shows effects of Reynolds number on particle deposition velocity in duct airflow with and without CHT. The temperature difference between inlet hot air and cool wall ΔT is 100 K for all the cases. For CHT cases, the thermal conductivity ratio λ_s/λ_f is 10 and the solid and fluid width ratio B/H is 1. It can be observed that particle deposition velocity firstly decreases slightly, then dramatically increases and finally keeps constant with the increase of particle relaxation time when ΔT = 0 K. When ΔT = 100 K, particle deposition velocities are obviously increased by thermophoresis for small particles (τ_p^+<20). However, deposition velocities of large particles (τ_p^+>20) almost keep the same. It can be found that the critical particle size is 28 μm. Therefore, thermophoresis has significant influences on deposition characteristics of small particles while almost no effects on large particle deposition. The maximum increase ratio of deposition velocity can reach 7.5 for ΔT = 100 K and Re = 3425, when particle size is 1 μm. Moreover, particle deposition velocity is decreased for small particles (τ_p^+<20) but keeps the same for large particles (τ_p^+>20) when CHT is considered, as shown in Fig. 5. This indicates that CHT only has influence on deposition behaviors of small particles, as thermophoresis is one of the dominant mechanisms for deposition of small particles. When Re is higher, it can be seen that the effects of CHT on particle deposition velocity reduction is larger. This is because the thermal convection in fluid region becomes more intense for higher Re case. Furthermore, particle deposition velocity is significantly increased for all sizes of particles when Re increases. The turbulent vortex will be greatly enhanced for higher Re case. Thus more particles will be captured by flow eddies and entrained to wall surface for deposition.

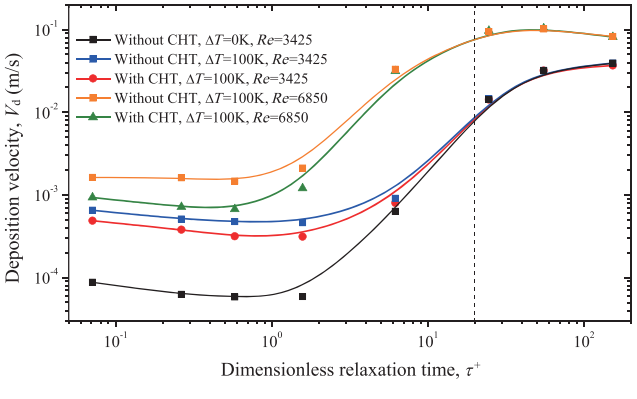

Fig. 5 Effects of Reynolds number on particle deposition in duct flow with and without CHT

Thermophoretic deposition behaviors of particles are greatly influenced by air temperature fields. Figure 6 shows effects of Reynolds number on thermal fields in duct flow with and with CHT. The temperature difference between inlet hot air and cool wall is 100 K in the figure. It can be seen that thermal boundary layer for Re = 3425 is much thicker than that for Re = 6850. Therefore, the temperature variety in the near-wall region is much dramatic for high Re case. The thermophoretic force of particle is directly proportional with the temperature gradient. As the thermophoretic force is towards to the wall in the present study, the dramatic temperature variety is useful for thermophoretic deposition. Moreover, when CHT is considered, it can be found that the temperature of inner wall surface is higher than 300 K due to the conjugate thermal conduction of solid wall domain. Therefore, the wall-normal temperature difference in the airflow region for CHT case is reduced compared with no CHT case. This would reduce the thermophoresis effect of particles, especially for small particles. Thus deposition velocity of small particles is greatly decreased by considering CHT. Besides, the thermal convection in fluid domain and thermal conduction in solid domain are both enhanced for higher Re case. Therefore, thermophoretic deposition of small particles is more reduced by CHT in condition of higher flow velocity.

4.3 Effects of temperature difference on particle deposition with and without CHT

Effects of temperature difference on particle deposition with and without CHT were displayed in Fig. 7. The flow Reynolds number is 3425. The thermal conductivity ratio and width ratio of solid and fluid domain are 10 and 1, respectively. The temperature difference ΔT between inlet hot air and cool wall is 0, 50 or 100 respectively. It can be found that thermophoretic deposition is obvious for small particles but very limited for large particles for different ΔT. The critical particle diameter is both 28 μm, no matter the ΔT is 50 or 100 K. This indicates that the influencing range of particle diameter is the same when temperature difference changes. Moreover, deposition velocity of small particles obviously increases due to enhancement of thermophoretic deposition when temperature difference increases. Thus temperature difference is a dominant factor for thermophoresis effect. When CHT was considered, deposition velocity is decreased for small particles for the both cases (ΔT = 50 K and ΔT =100 K). The conclusions are consistent with the discussion in the Section 3.2.

Figure 8 shows effects of temperature difference on thermal fields in duct flow with and with CHT. The flow Reynolds number is 3425. The thermal conductivity ratio and width ratio of solid and fluid domain are 10 and 1,

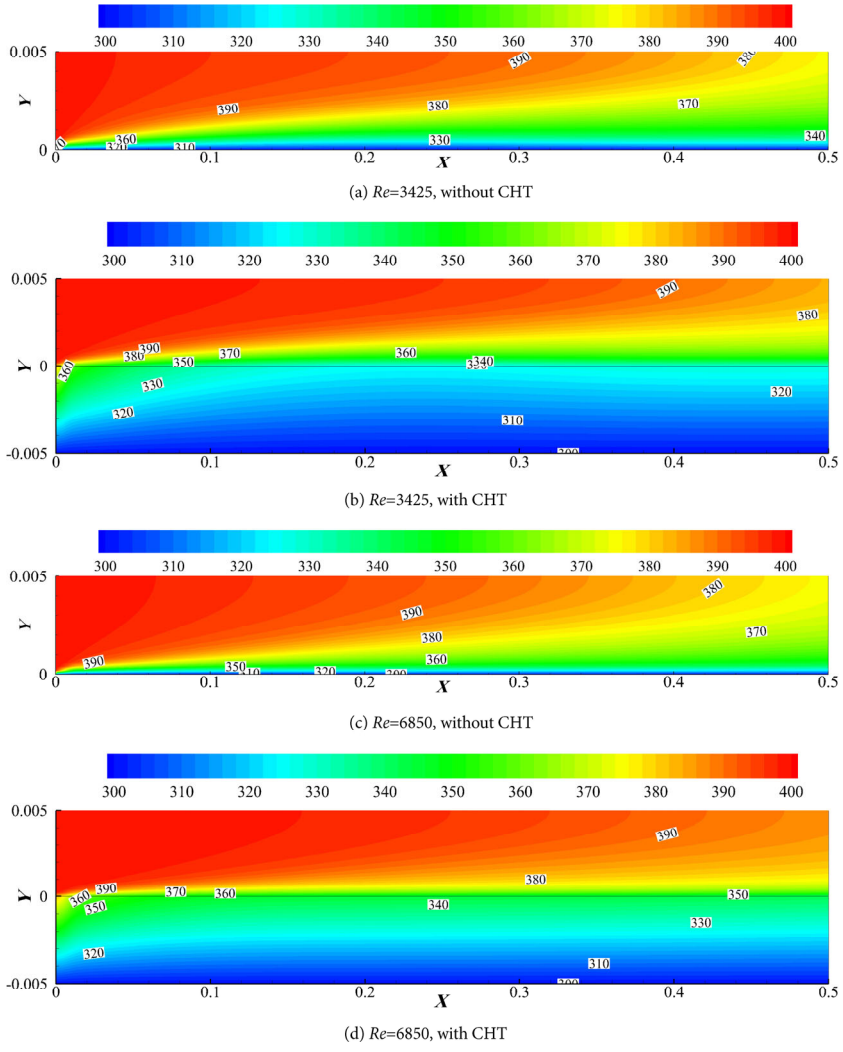

Fig. 6 Effects of Reynolds number on thermal fields in duct flow with and with CHT

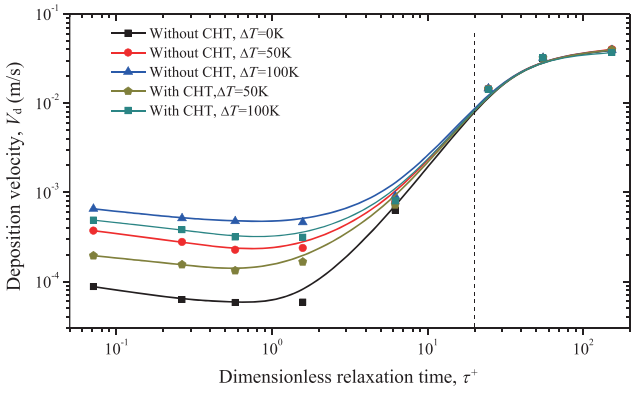

Fig. 7 Effects of temperature difference on particle deposition in duct flow with and with CHT

respectively. The temperature difference ΔT between inlet hot air and cool wall is 50 or 100 respectively. From the figure, it can be observed that the thermal distribution patterns for different ΔT cases are quite similar, although the actual temperature is higher for large ΔT case. The temperature variety for ΔT =100 K in the wall-normal direction is higher compared with the case of ΔT = 50 K. Therefore, thermophoretic particle deposition is increased when ΔT increases. When CHT was considered, it can be found that the temperature distribution patterns are also similar for different ΔT cases. Thus CHT has the same influence on thermophoresis of particles when ΔT changes.

4.4 Effects of thermal conductivity ratio on particle deposition with CHT

The thermal conductivity ratio of solid and fluid domain may have significant influence on CHT, and then further affect particle deposition characteristics. Effects of thermal conductivity ratio on particle deposition in duct flow with CHT were displayed in Fig. 9. The flow Reynolds number is 3425. The width ratio of solid and fluid domain is 1 and

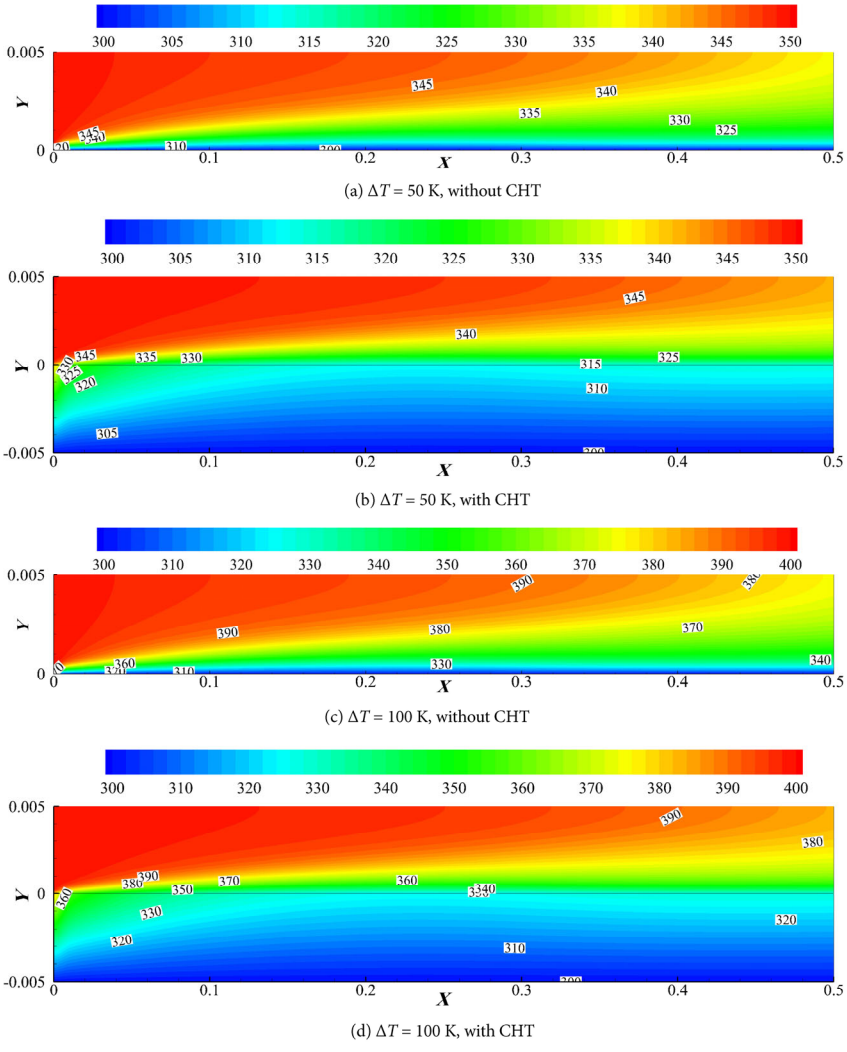

Fig. 8 Effects of temperature difference on thermal fields in duct flow with and with CHT

the temperature difference ΔT between inlet hot air and cool wall is 100. The thermal conductivity ratio of solid and fluid region λ_s/λ_f is 1, 10 or 100, respectively. It can be found that particle deposition velocity profile almost doesn't change when thermal conductivity ratio is 100, as shown in Fig. 9. However, particle deposition velocity is dramatically decreased for small particles (τ_p^+ <20) when thermal conductivity ratio is 10 or 1. The deposition velocity of large particles (τ_p^+ >20) keeps the same when thermal conductivity ratio changes from 1 to 100. These indicate that CHT has great influence on deposition velocity of small particles when thermal conductivity of solid domain is close to that of fluid domain. Nevertheless, deposition behaviors of large particles are not modified by CHT with small thermal conductivity ratio.

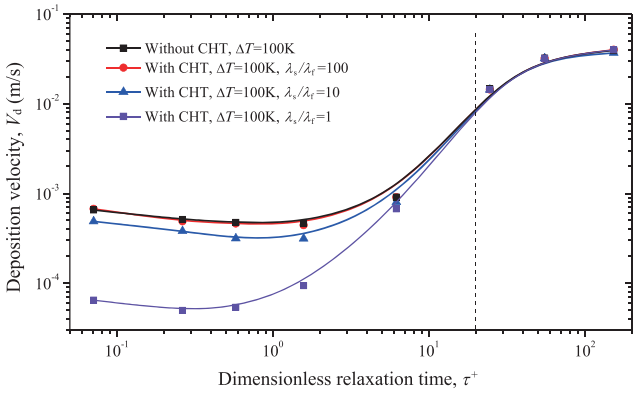

Fig. 9 Effects of thermal conductivity ratio on particle deposition in duct flow with CHT

Figure 10 illustrates effects of thermal conductivity ratio on thermal fields in duct flow with CHT. The flow Reynolds number is 3425. The width ratio of solid and fluid domain is 1 and the temperature difference ΔT between inlet hot air and cool wall is 100. The thermal conductivity ratio of solid and fluid region λ_s/λ_f is 1, 10 or 100, respectively. It can be seen that the temperature distributions for different thermal conductivity ratio are quite different. When thermal

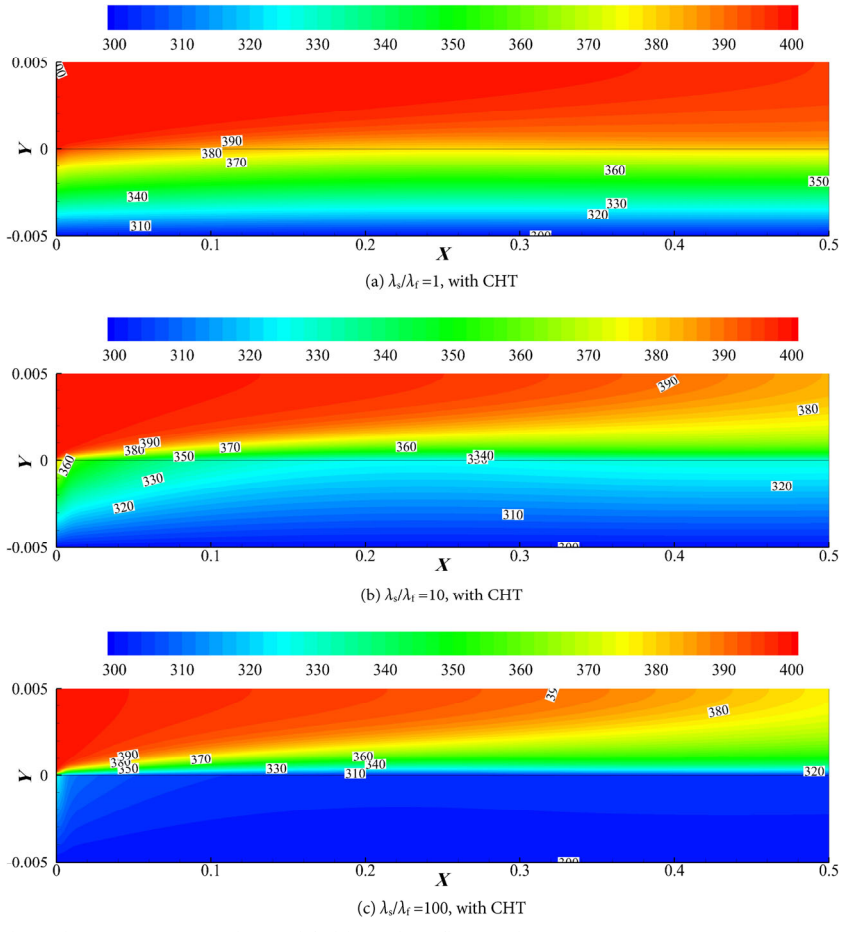

Fig. 10 Effects of thermal conductivity ratio on thermal fields in duct flow with CHT

conductivity ratio is 100, the temperature in solid domain is close to 300 K and the temperature variety is small. This indicates that thermal conduction in solid wall is very fast due to high thermal conductivity. The temperature field in fluid region is almost the same from the case without CHT. Thus particle deposition velocity doesn't change when thermal conductivity ratio is 100. However, temperature difference in solid domain is dramatically increased when thermal conductivity ratio decreases to 10 or 1. The temperature distribution in fluid region is greatly modified by CHT and temperature difference in wall-normal direction is decreased because of thermal conduction in solid wall. Thus particle deposition velocity is decreased with decrease of thermal conductivity ratio.

4.5 Effects of solid and fluid width ratio on particle deposition with CHT

Effects of solid and fluid width ratio on particle deposition in duct flow with CHT were illustrated in Fig. 11. The flow Reynolds number is 3425. The temperature difference ΔT between inlet hot air and cool wall is 100 and the thermal conductivity ratio of solid and fluid region is 10. The width ratio of solid and fluid domain is 1, 2 or 4 respectively. It can be found that particle deposition velocity uniformly decreases with the increase of width ratio B/H, when particle relaxation time is less than 20. However, deposition velocity doesn't change by CHT when particle relaxation time is larger than 20. When width ratio B/H is 1, the maximum decrease ratio of particle deposition velocity is 75% for 1 μm particles.

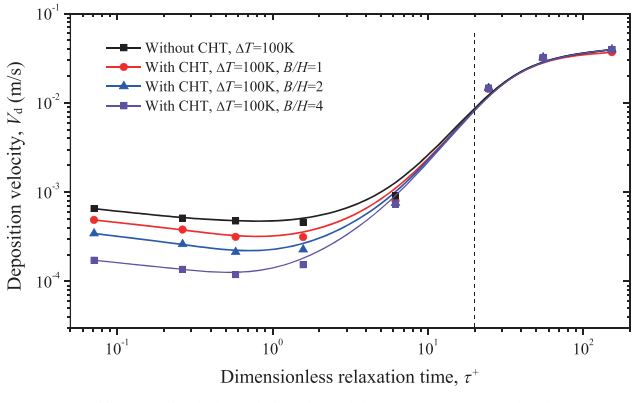

Fig. 11 Effects of solid and fluid width ratio on particle deposition in duct flow with CHT

Nevertheless, the maximum decrease ratio of deposition velocity can reach 26% for 1 μm particle when width ratio B/H is 4.

Moreover, Fig. 12 displays effects of solid and fluid width ratio on particle deposition in duct flow with CHT. The flow Reynolds number is 3425. The temperature difference ΔT between inlet hot air and cool wall is 100 and the thermal conductivity ratio of solid and fluid region is 10. The width ratio of solid and fluid domain is 1, 2 or 4 respectively. It can be found that the temperature fields are obviously changed when width ratio B/H is different. The temperature is significantly increased when width ratio B/H increases. On the contrary, the temperature difference of fluid domain in wall-normal direction is decreased with increase of width ratio B/H. Therefore, particle deposition velocity would decrease when width ratio B/H is higher.

5 Conclusions

Particle deposition with thermophoresis in turbulent duct airflow with and without CHT was studied by $\overline{v'^2} - f$ model and discrete particle model with a modified discrete random walk method. The grid independence test and numerical verification were conducted in the study. The effects of flow Reynolds number, temperature difference between inlet hot air and cool wall, thermal conductivity ratio and width ratio of solid and fluid domain on particle deposition velocity were investigated and analyzed in details. Moreover, the thermal fields for both solid and flow domain in different conditions were analyzed and discussed in the study. The following conclusions can be drawn,

1) The CHT reduces deposition velocity of small particles (τ_p^+ <20) but no effect on large particle deposition (τ_p^+ >20), as thermophoresis is one of the dominant mechanisms for deposition of small particles. The effects of CHT on particle deposition velocity become more intense when Re is higher, as thermal convection in fluid domain and thermal conduction in solid domain are both enhanced for higher Re case.
2) Deposition velocity of small particles (τ_p^+ <20) obviously increases for both CHT and no CHT cases due to enhancement of thermophoretic deposition when temperature difference increases. The wall-normal temperature variety for higher ΔT is more dramatic compared with

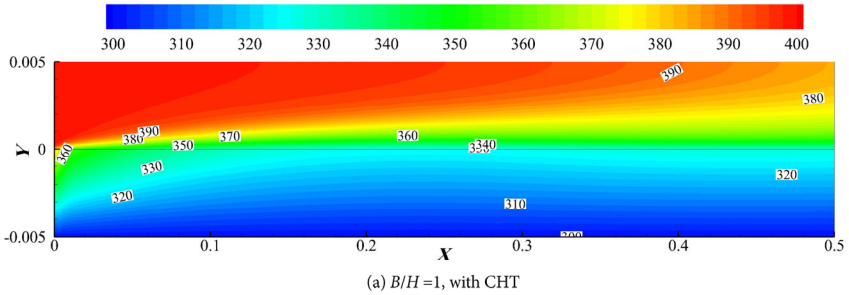

(a) B/H =1, with CHT

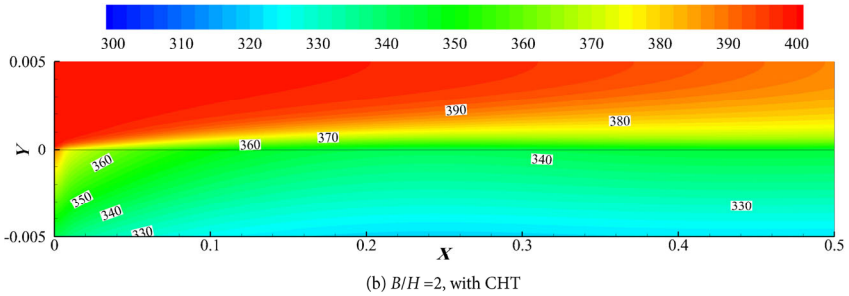

(b) B/H =2, with CHT

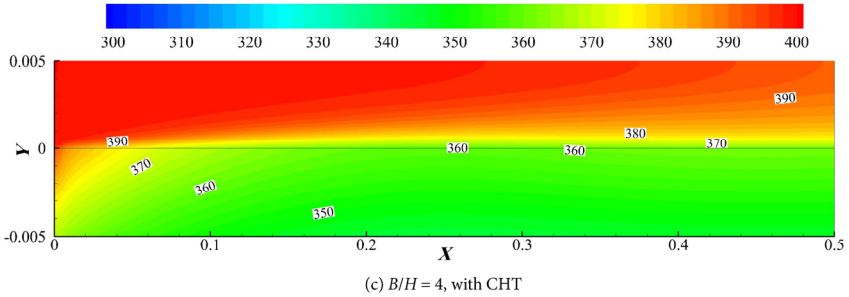

(c) B/H = 4, with CHT

Fig. 12 Effects of solid and fluid width ratio on thermal fields in duct flow with CHT

the case of lower ΔT. Therefore, thermophoretic particle deposition is increased when ΔT increases.

3) The CHT has great influence on deposition velocity of small particles (τ_p^+ <20) when thermal conductivity of solid domain is close to that of fluid domain. Nevertheless, deposition behaviors of large particles are not modified by CHT even with small thermal conductivity ratio. This is because temperature difference is dramatically increased in solid domain while greatly decreased in fluid domain when thermal conductivity ratio decreases.
4) Particle deposition velocity uniformly decreases with the increase of width ratio B/H when τ_p^+ <20. The temperature difference of fluid domain in wall-normal direction is decreased with increase of width ratio B/H. Therefore, particle deposition velocity would decrease when width ratio B/H is higher.
5) For all the cases, thermophoresis only influences deposition behaviors of small particles but doesn't affect large particle deposition. The maximum increase ratio of deposition velocity can reach 7.5 for ΔT = 100 K and Re=3425, when particle size is 1 μm. The critical particle relaxation time τ_p^+ is 20, which is the same for all the cases in this study. The corresponding particle diameter is 28 μm.

Therefore, CHT has significant influences on particle deposition characteristics in turbulent duct flow. The numerical simulation would over-predict the deposition velocity on the cooler walls if the CHT is not considered. Moreover, the influencing factors studied in the present study can be used to modify thermophoretic deposition of particles in realistic engineering application.

Acknowledgements

The authors appreciate the financial supports provided by the National Key Research and Development Program (No. 2017YFE0116100), the"Xinghua Scholar Talents Plan"of South China University of Technology (D6191420) and the Fundamental Research Funds for the Central Universities (D2191930). It is also supported by the National Science Fund for Distinguished Young Scholars (No. 51425601) and the Science and Technology Planning Project of Guangdong Province: Guangdong-Hong Kong Technology Cooperation Funding Scheme (TCFS), No. 2017B050506005.

References

Bakanov SP (1991). Thermophoresis in gases at small Knudsen numbers. *Aerosol Science and Technology*, 15: 77–92.

Chen S, Gong W, Yan YY (2018). Conjugate natural convection heat transfer in an open-ended square cavity partially filled with porous media. *International Journal of Heat and Mass Transfer*, 124: 368–380.

Cheng YS (1997). Wall deposition of radon progeny and particles in a spherical chamber. *Aerosol Science and Technology*, 27: 131–146.

Dong YH, Chen LF (2011). The effect of stable stratification and thermophoresis on fine particle deposition in a bounded turbulent flow. *International Journal of Heat and Mass Transfer*, 54: 1168–1178.

Durbin PA (1995). Separated flow computations with the k-epsilon-v-squared model. *AIAA Journal*, 33: 659–664.

El-Shobokshy MS (1983). Experimental measurements of aerosol deposition to smooth and rough surfaces. *Atmospheric Environment (1967)*, 17: 639–644.

FLUENT (2009). FLUENT 12.0 User's Guide. Lebanon, NH, USA: FLUENT Inc.

Friedlander SK, Johnstone HF (1957). Deposition of suspended particles from turbulent gas streams. *Industrial & Engineering Chemistry*, 49: 1151–1156.

Gao N, Niu J, He Q, Zhu T, Wu J (2012). Using RANS turbulence models and Lagrangian approach to predict particle deposition in turbulent channel flows. *Building and Environment*, 48: 206–214.

He C, Ahmadi G (1998). Particle deposition with thermophoresis in laminar and turbulent duct flows. *Aerosol Science and Technology*, 29: 525–546.

Lai ACK (2002). Particle deposition indoors: A review. *Indoor Air*, 12: 211–214.

Lee KW, Gieseke JA (1994). Deposition of particles in turbulent pipe flows. *Journal of Aerosol Science*, 25: 699–709.

Lee BU, Sub Byun D, Bae GN, Lee JH (2006). Thermophoretic deposition of ultrafine particles in a turbulent pipe flow: Simulation of ultrafine particle behaviour in an automobile exhaust pipe. *Journal of Aerosol Science*, 37: 1788–1796.

Liu BYH, Agarwal JK (1974). Experimental observation of aerosol deposition in turbulent flow. *Journal of Aerosol Science*, 5: 145–155.

Liu R, You C, Yang R, Wang J (2010). Direct numerical simulation of kinematics and thermophoretic deposition of inhalable particles in turbulent duct flows. *Aerosol Science and Technology*, 44: 1146–1156.

Lu H, Lu L (2015a). A numerical study of particle deposition in ribbed duct flow with different rib shapes. *Building and Environment*, 94: 43–53.

Lu H, Lu L (2015b). Effects of rib spacing and height on particle deposition in ribbed duct air flows. *Building and Environment*, 92: 317–327.

Lu H, Lu L (2016). CFD investigation on particle deposition in aligned and staggered ribbed duct air flows. *Applied Thermal Engineering*, 93: 697–706.

Lu H, Lu L, Jiang Y (2017). Numerical study of monodispersed particle deposition rates in variable-section ducts with different expanding or contracting ratios. *Applied Thermal Engineering*, 110: 150–161.

Majlesara M, Salmanzadeh M, Ahmadi G (2013). A model for particles deposition in turbulent inclined channels. *Journal of Aerosol Science*, 64: 37–47.

Olufade AO, Simonson CJ (2018). Application of indirect non-invasive methods to detect the onset of crystallization fouling in a liquid-to-air membrane energy exchanger. *International Journal of Heat and Mass Transfer*, 127: 663–673.

Partankar SV (1980). Numerical Heat Transfer and Fluid Flow. Washington, DC: Hemisphere Publishing Corporation.

Postma AK, Schwendiman LC (1960). Studies in micrometrics: I. Particle deposition in conduits as a source of error in aerosol sampling. Report HW-65308. Richland, WA, USA: Hanford Laboratory.

Romay FJ, Takagaki SS, Pui DYH, Liu BYH (1998). Thermophoretic deposition of aerosol particles in turbulent pipe flow. *Journal of Aerosol Science*, 29: 943–959.

Shimada M, Okuyama K, Asai M (1993). Depostition of submicron aerosol particles in turbulent and transitional flow. *AIChE Journal*, 39: 17–26.

Sippola MR, Nazaroff WW (2004). Experiments measuring particle deposition from fully developed turbulent flow in ventilation ducts. *Aerosol Science and Technology*, 38: 914–925.

Thakurta DG, Chen M, McLaughlin JB, Kontomaris K (1998). Thermophoretic deposition of small particles in a direct numerical simulation of turbulent channel flow. *International Journal of Heat and Mass Transfer*, 41: 4167–4182.

Tian L, Ahmadi G (2007). Particle deposition in turbulent duct flows—Comparisons of different model predictions. *Journal of Aerosol Science*, 38: 377–397.

Wang X, You C, Liu R, Yang R (2011). Particle deposition on the wall driven by turbulence, thermophoresis and particle agglomeration in channel flow. *Proceedings of the Combustion Institute*, 33: 2821–2828.

Wells C, Chamberlain C (1967). Transport of small particles to vertical surfaces. *British Journal of Applied Physics*, 18: 1793–1799.

Zhang LZ (2015). Transient and conjugate heat and mass transfer in hexagonal ducts with adsorbent walls. *International Journal of Heat and Mass Transfer*, 84: 271–281.

Zhang Z, Chen Q (2009). Prediction of particle deposition onto indoor surfaces by CFD with a modified Lagrangian method. *Atmospheric Environment*, 43: 319–328.

Zhao B, Zhang Y, Li X, Yang X, Huang D (2004). Comparison of indoor aerosol particle concentration and deposition in different ventilated rooms by numerical method. *Building and Environment*, 39: 1–8.

Zhao B, Wu J (2006). Modeling particle deposition from fully developed turbulent flow in ventilation duct. *Atmospheric Environment*, 40: 457–466.

Zhao B, Yang C, Yang X, Liu S (2008). Particle dispersion and deposition in ventilated rooms: Testing and evaluation of different Eulerian and Lagrangian models. *Building and Environment*, 43: 388–397.